INVESTIGATION OF AIRBORNE LIDAR FOR AVOIDANCE OF WINDSHEAR HAZARDS

Russell Targ
Lockheed Missiles & Space Company, Inc.
Research & Development Division
Palo Alto, California 94304

and

Roland L. Bowles
NASA Langley Research Center
Hampton, Virginia 23665-5225

Abstract

A generalized windshear hazard index is defined, which is derived from considerations of wind conditions at the present position of an aircraft and from remotely sensed information along the extended flight path. Candidate airborne sensor technologies based on microwave Doppler radar, Doppler lidar, and infrared radiometric techniques are discussed in the context of overall system functional requirements. Initial results of a performance and technology assessment study for competing lidars are presented. Based on a systems approach to the windshear threat, lidar appears to be a viable technology for windshear detection and avoidance, even in conditions of moderately heavy precipitation. The proposed airborne CO_2 and Ho:YAG lidar windshear-detection systems analyzed in this paper can give the pilot information about the line-of-sight component of windshear threat from his present position to a region extending 1 to 3 km in front of the aircraft. This constitutes a warning time of 15 to 45 seconds. The technology necessary to design, build, and test such a brassboard 10.6-μm CO_2 lidar is now available. However, for 2-μm systems, additional analytical and laboratory investigations are needed to arrive at optimum 2-μm rare-earth-based laser crystals.

Nomenclature

B	=	system bandwidth
d	=	telescope diameter
D	=	aircraft drag force
E	=	total aircraft energy (or laser pulse energy)
F	=	aircraft specific hazard index (nondimensional)
g	=	acceleration of gravity
h_p	=	aircraft potential altitude (energy height)
h	=	aircraft altitude
$K(R)$	=	round-trip extinction for range R
L	=	distance between adjacent range gates
R	=	range of return
T	=	aircraft thrust force
V	=	aircraft airspeed
W	=	aircraft weight
W_h	=	vertical component of inertial wind
W_x	=	horizontal component of inertial wind
β	=	backscatter cross section
γ	=	flight path angle relative to air mass
λ	=	laser wavelength
η	=	detection and mixing efficiency
τ	=	forward-look alert time
∇	=	gradient operator

1. Background and Introduction

Low-altitude windshear is recognized by the commercial aviation industry as a major hazard. In the United States, during the period 1964 to 1985, windshear has been a contributing factor in at least 26 civil transport accidents and 3 incidents involving 500 fatalities and over 200 injuries. Numerous methods of reducing the low-altitude windshear hazard have been proposed by the airlines, airframe manufacturers, and the Government. The Federal Aviation Administration (FAA), as lead agency for civil aviation safety, has established an integrated windshear program plan which addresses the windshear problem through focused research and development efforts over a 5-year period. The National Aeronautics and Space Administration (NASA) has responded by signing a memorandum of agreement with the FAA (July 1986) to pursue a cooperative research program which addresses technical factors related to airborne detection, avoidance, and survivability of severe windshear atmospheric conditions. Key elements of the NASA research effort include characterization of windshear phenomena in the aviation context, airborne remote-sensor technology that provides forward-looking avoidance capability, and flight-management system concepts that promote risk-reduction piloting through timely and accurate transfer of information to flight crews. The NASA research thrust is directed at developing system concepts which embrace forward-looking sensor technology, thereby providing the flight crew with awareness of the presence of windshear with enough time to avoid the affected area and escape from the encounter.

This paper emphasizes the analysis of competing lidars for use in an airborne forward-looking system, to enable aircraft to avoid the hazards of low-altitude windshear. The analysis includes a definition of lidar sensor requirements, the formulation of a system to meet these requirements, and an investigation and simulation of the capabilities and limitations of such a system, together with recommendations identifying the most feasible and cost-effective laser for use in a lidar system for windshear detection and avoidance.

The two lidar systems investigated, solid-state Ho:YAG at 2.1 μm and CO_2 at 10.6 μm, appear able to meet the windshear warning requirements as determined by computer simulations of the 1985 Dallas/Fort Worth microburst event. The performance of Ho:YAG is potentially superior to that of the CO_2 lidar, but Ho:YAG is far from being available at this time. On the other hand, the CO_2 technology is quite mature, and has been tested extensively in both airborne and ground-based wind-field mapping applications.

2. The Threat From Windshear

National attention has focused on the critical problem of detecting and avoiding windshear since the crash on August 2, 1985, of Delta Air Lines Flight 191, a Lockheed L-1011, at the Dallas/Fort Worth International Airport. Other crashes and near misses caused by windshear have occurred almost annually.

The hazard of windshear arises principally from its deceptive nature: In a windshear situation, from a microburst or any other source, the pilot is confronted with a performance-increasing headwind, followed a few seconds later by a powerful, performance-decreasing tailwind. To cope with the headwind, the pilot may take actions to prevent the plane from climbing. These actions are then compounded by the lack of lift caused by the tailwind and downdraft, so that it may be impossible to keep the plane in the air. The downburst shown in Fig. 1 can be entirely invisible to the pilot and the ground controllers, and it need not be associated with any rain on the ground. In a NASA/FAA study of 186 windshear occurrences in 1983, the average change in wind speed was approximately 40 knots.[1]

The NASA/FAA Joint Airport Weather Study (JAWS)[1] observed and measured windshears at the Denver/Stapleton Airport over a 3-month period. The principal finding confirmed that "... low-altitude wind variability (or windshear) presents an infrequent but highly significant hazard to aircraft landing or taking off." From analysis of aircraft accidents where low-altitude windshear was a factor, it appears that the greatest hazards are caused by downdrafts and outflows produced by convective storms.

Pilots now receive inconsistent windshear warnings that are of questionable reliability. The ground-based data from anemometers must first be interpreted by trained meteorologists. The tower attempted to warn Flight 191 of windshear a full 2 min after it crashed. The *Windshear Training Aid*[2] produced by the NASA/FAA Integrated Program in 1986 carries the warning, "Maximum windshear capability of jet transports at heavy weight, for a windshear encounter at a critical location, is 40 to 50 knots wind-speed change. Some windshears cannot be escaped successfully [once they are actually entered]!". For this reason it is essential to emphasize avoidance rather than recovery. An onboard forward-looking windshear-avoidance system can warn the pilot, at the location marked "windshear entry" in Fig. 1, that he is approaching a wind hazard. When the plane is at the location "recover or crash," it can be too late to inform the pilot that he is in windshear.

3. Requirements for an Airborne Windshear Detection System

The fundamental requirement for a forward-looking, airborne windshear detection system is realtime remote sensing. This implies the ability to reliably measure line-of-sight and vertical components of wind velocity and to alert the crew when they are approaching a windshear hazard. The system should monitor the approach path, the runway, and the takeoff path, in both rain and clear-air conditions. This alert should be provided with enough warning time to allow the pilot to increase the energy of the plane and safely transit or avoid the microburst. The quantitative technical requirements are given in Table 1.

Table 1. Quantitative Technical Requirements

Minimum sensing range	1 to 3 km
Advance warning time	15 to 40 s
Range resolution	0.3 km
Velocity resolution	Approximately 1 m/s

Fig. 1. The windshear problem.

There are additional functional requirements for any airborne system: It must not interfere with other instruments on the aircraft; it should be as small as possible; it should operate reliably in an aircraft environment for 2000 hours with little or no maintenance; and it should not require any expendable supplies that would have to be replenished. All these factors should work together to make a system that is almost free from false or nuisance alarms. The first specific hazard that should trigger a windshear alarm is a performance-decreasing wind (tailwind) which increases its velocity at a rate of 2 knots/s in the direction of travel of the aircraft. A second threatening condition is the downburst, which is considered a hazard when the vertical velocity reaches 1500 ft/min. A numerical hazard index "F" has been derived by NASA using both these factors, where $F > 0.1$ is considered a potential aircraft hazard.

4. Definition of Hazard Index

The key to the development of airborne windshear detection, warning, and avoidance systems is the identification of a hazard index. This index should exhibit a functional dependence on atmospheric states that can be reliably sensed, and scale with available aircraft performance in such a way that the index predicts impending flight-path deterioration. The hazard index must also account for factors such as the statistical nature of the windshear threat, fusion of present position and "forward-looking" sensor capabilities, and the development of objective methods for determining system warning thresholds which consider the potential for nuisance alerts. A hazard index which has the above properties and is based on accepted fundamentals of flight mechanics and current state of knowledge of windshear phenomena has been derived.

An analysis was conducted which revealed the importance of aircraft energy balance for flight in spatially and temporally varying windfields. This energy-state analysis showed that aircraft motions should be referenced to the accelerated and nonhomogenous airmass which typifies windshear phenomena. The concepts of airplane total energy and rate of change of total energy are useful in interpreting the impact of windshear on aircraft performance. The airplane total energy is defined as the sum of the air-mass relative kinetic energy and the inertial potential energy. Air-mass kinetic energy is used since only airspeed, not ground speed, describes the airplane's ability to climb or maintain altitude. Inertial potential energy is likewise used since it is altitude above the ground that is useful to the airplane.

Therefore, airplane total specific energy (energy per unit weight), or *potential* altitude, is defined as:

$$h_p = \frac{E}{W} = \frac{V^2}{2g} + h \tag{1}$$

where V is airspeed, W is aircraft weight, and h is aircraft altitude. The rate of change of specific energy—also defined as the potential rate of climb of the airplane, assuming negligible energy loss when trading airspeed for climb rate—is given by:

$$\dot{h}_p = \frac{\dot{E}}{W} = \frac{V}{g}\dot{V} + \dot{h}. \tag{2}$$

When combined with appropriate aircraft equations of motion,[3] the potential rate of climb given by Eq. (2) reduces to:

WINDSHEAR "HIT"

$$\dot{h}_p = \frac{\dot{E}}{W} = \left\{\frac{T-D}{W} - \left[\frac{\dot{W}_x}{g}\cos\gamma + \frac{\dot{W}_h}{g}\sin\gamma - \frac{W_h}{V}\right]\right\}V; \tag{3}$$

where $(T - D)/W$ is the ratio of aircraft thrust minus drag to weight, W_x and W_h are the horizontal and vertical wind velocity components, respectively, and γ is the flight-path angle relative to airmass.

The dot notation in Eq. (3) indicates the substantial derivative with respect to time, since the wind velocity components depend explicitly on aircraft position.

For representative numerical values of windshear gradients, and for flight-path angles compatible with stabilized flight, i.e., for $\gamma \approx 0$, the hazard index labeled as windshear "hit" in Eq. (3) is accurately approximated as

$$F = \frac{\dot{W}_x}{g} - \frac{W_h}{V} \tag{4}$$

and Eq. (3) takes the approximate form:

$$\dot{h}_p = \frac{\dot{E}}{W} = \left[\frac{T-D}{W} - F\right]V. \tag{5}$$

Equations (4) and (5) explicitly define the quantitative impact of windshear on aircraft energy state and the rate-of-climb capability. The analysis reveals that the rate of change of specific energy (potential climb rate) depends linearly on a nondimensional parameter F, which contains only information regarding air mass movement. Further analysis indicates that the subject parameter can be physically interpreted as the loss or gain in available excess thrust-to-weight ratio due to downdrafts, updrafts, and horizontal windshear, thus providing an aircraft-specific index on which to base annunciated warnings.

The derived hazard index given by Eq. (4), referred to as the F-factor, exhibits the following properties:

1. It scales with available aircraft performance in such a way as to predict impending flight-path deterioration.
2. It shows a functional dependence on atmospheric states that can be reliably sensed.
3. It is applicable to both in-situ and remotely sensed windshear information.
4. It is compatible with stringent nuisance-alarm requirements.

Positive values of F indicate a performance-decreasing situation for the aircraft, whereas negative values indicate a performance-increasing condition due to atmospheric disturbance. Considering jet transports in take-off configuration and the current state of knowledge regarding windshear phenomena, typical numerical

values for the terms under hazardous conditions making up the F-factor are:

$$0.1 \le \frac{T-D}{W} \le 0.3; \quad |\dot{W}_x| \le 0.3\,g; \quad \left|\frac{W_h}{V}\right| \le 0.25.$$

Note that a headwind loss of $\dot{W}_x = 0.1\,g$ (2 knots/s) has the same impact on aircraft performance (F value) as a downdraft W_h = -15 knots (-1500 ft/min), considering a reference airspeed of 150 knots. Figure 2 shows the "safe operations" conditions as a function of the F-factor variables.

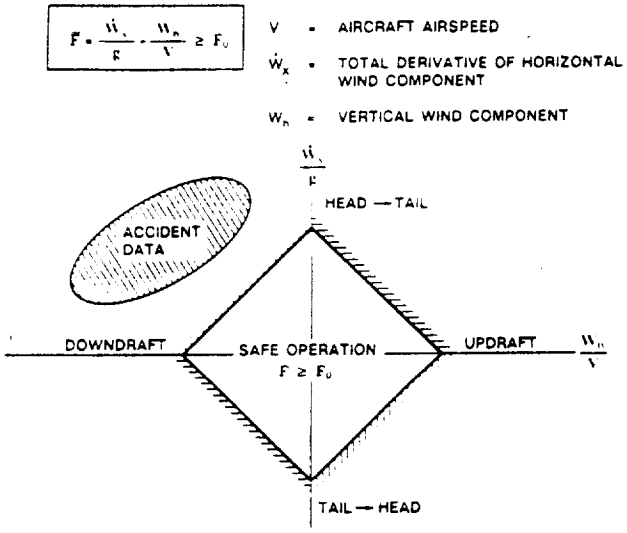

Fig. 2 Definition F-factor hazard index.

A possible airborne windshear detection, warning, and avoidance system architecture, which flows from the application of the F-factor concept, is shown in Fig. 3. The proposed architecture is compatible with a single-tier warning system (no amber caution) and provides for fusion of "present position" information, F(t), with "forward look" information, $F(t + \tau)$. The prediction interval τ is determined by a preselected and interrogated range gate divided by current aircraft ground speed. A preset hazard threshold F_0 is incorporated, which, when exceeded below a specified aircraft altitude, provides an alert to the flight crew. Any combination of horizontal windshear and/or vertical wind that results in F less than the threshold value indicates safe aircraft

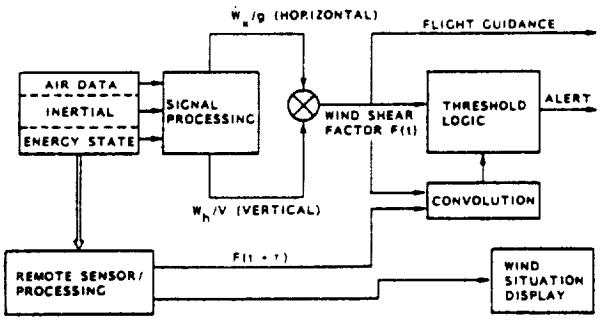

Fig. 3 Fusion of present-position and predictive information.

operation in relation to available excess thrust-to-weight ratio for that aircraft. A threshold exceedance that persists for a sufficient period of time warrants the annunciation of a windshear warning, which indicates to the crew that the affected area should be avoided or an escape maneuver should be initiated. The alert and warning threshold is determined by considering the maximum permissible F in relation to available aircraft performance capability while minimizing potential for nuisance warnings. Research indicates that threshold values for F between 0.1 and 0.15 are representative for landing and take-off phases of flight for jet transport aircraft, considering factors such as aircraft type, configuration, and range of gross weights. Figure 4 illustrates average values for windshear F-factors derived from five aircraft accidents. The data presented indicate that, in all cases, the average F-factor exceeded the ability of the airplane at maximum weight to accelerate in level flight.

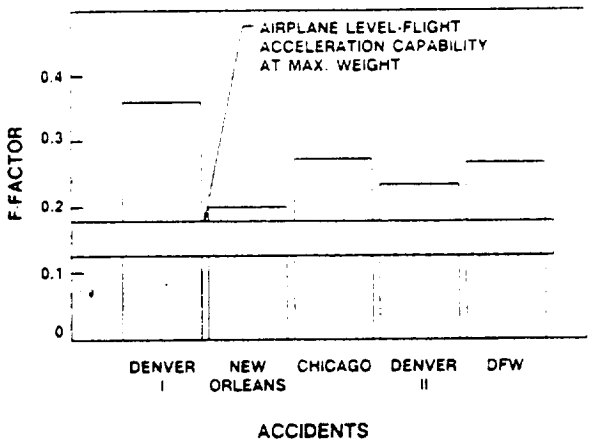

Fig. 4 Accident windshear F-factors compared to airplane capabilities.

The F-factor concept can be extended to forward-looking sensors through utilization of spatial wind measurements along a given line-of-sight direction, a characteristic which is typical for pulsed-Doppler detection and ranging systems. The substantial derivation expressed in Eq. (4), assuming a "frozen wind field" hypothesis, can be approximated as:

$$\dot{W}_x = \nabla W_x \cdot V_I + \frac{\partial W_x}{\partial t} = \frac{\partial W_x}{\partial X} V \qquad (6)$$

where V_I is the inertial velocity vector of the aircraft. If Eq. (6) is substituted into Eq. (4) and the result linearized about the ith. range gate along a ray of the forward-look sensor, one obtains the recursion

$$F(i+1) = F(i) + \frac{V}{gL}\,[W_x(i+2) - 2W_x(i+1) + W_x(i)] - \frac{W_h(i+1)}{V} \qquad (7)$$

The quantity L is defined as the distance between any two adjacent range gates along a line-of-sight ray of the

active sensor. Typical values for L are between 150 m and 500 m, depending on sensor pulse width. The realtime calculation of Eq. (7) predicts the distribution of hazard index based on absolute wind measurements at predetermined range gates. Note that $F(0)$, $W_t(0)$, and $W_n(0)$, which can be determined from present position *in situ* measurements, are required to initialize the iteration. Application of the algorithm described above, in a variety of simulation studies, has demonstrated the need for presmoothing the spatial wind measurements in order to suppress small-eddy turbulence, otherwise an unacceptable incidence of nuisance warnings may occur.

5. Approaches to Airborne Windshear Detection

5.1 Lidar Systems

For more than two decades, optical heterodyne detection has been successfully used to measure the frequency of Doppler-shifted laser light scattered from moving aerosols. This technique has been pioneered by many researchers, including those working with both NASA and NOAA. Although wind-velocity measurements are routinely made with good accuracy to ranges of more than 10 km in clear air, the range is seriously degraded by rain. The attenuation from radiation in the infrared is approximately 9 dB/km per inch of rain per hour.[4] Thus, a moderate-size airborne lidar system, which may have 3- to 5-km range in clear air, will have its range reduced to 1 km in a rain of 3 in./h, such as one might find in the core of a wet microburst. However, even under these severe conditions, 14 s of advance warning can be provided.

Although the subject of this paper is the analysis of lidar approaches to windshear detection, it is useful to put lidar into context with two other candidate systems which are presently under active development to meet this goal.

5.2 Microwave Systems

High-power ground-based Doppler radars operating at C-band and X-band are able to measure wind velocity at ranges of 10 to 20 km by measuring the scattered radiation primarily from precipitation, ice crystals, or other debris in the air. Microwave systems receive only minimal returns from dry air. Although windshear is usually associated with violent thunderstorms in the southern United States, 80 percent of the observed windshear events in the Denver study (JAWS) were dry at ground level. If the wind data for the flight paths could be rapidly updated and made available to the pilots, flight safety could be greatly improved. A major problem with on-airport radars—and to an even greater extent airborne radars—is the appearance of ground clutter. For the airborne system, the clutter return from the moving terrain along the flight path has a much greater amplitude (approximately +60 dB) than, and a frequency in the same band as, the hoped-for Doppler return from the wind. In comparing airborne radars with the ground-based systems such as those participating in the successful JAWS measurements, one must take into account the reduction in transmitter power that such an airborne system will have available, as well as the reduced antenna aperture, leading to a beam divergence of several degrees. All these factors have a significant impact on the ultimate achievable signal-to-noise ratio (SNR) (−30 to −40 dB as compared with a ground-based system). Details regarding the NASA airborne windshear radar research efforts are found in Ref. 5.

5.3 Radiometer

Measurements indicate that there is a temperature gradient associated with the formation of a windshear. It appears that this gradient can be measured by an airborne infrared radiometer. The radiometers which have been used for this purpose measure emission from the 14-μm band of atmospheric CO_2. The technique compares emission from CO_2 in the immediate neighborhood of the aircraft to the emissions from the CO_2 in the air 2 or 3 km away. It is conjectured that the more negative this temperature gradient, the steeper the gust front causing it. Although it appears that radiometers of this type can detect temperature gradients associated with microbursts under favorable conditions, the question of nuisance alarms has not been addressed, since it has not yet been determined what other types of atmospheric phenomena cause similar gradients. Industry initiatives to exploit infrared technology for airborne windshear detection are discussed in Ref. 6.

6. Successful Lidar Wind-Velocity Measurements

Since early work in the 1970's, there have been many advances in airborne laser velocimetry. James Bilbro, at NASA's Marshall Space Flight Center, has successfully measured wind velocity from an aircraft using a modulated CO_2 continuous wave (cw) laser followed by a large high-power amplifier that produced 10 mJ at 10.6 μm.[7] Bilbro's Doppler lidar operates in clear air and has a range of more than 5 km. A compact and reliable laser system has been flight-tested for several years by J. Michael Vaughan of the Royal Signals and Radar Establishment.[8] His lidar used a cw CO_2 laser focused 300 m in front of the airplane to measure backscatter coefficients at many European and American test sites and airports. Vaughan also uses optical heterodyne detection to determine the plane's velocity from the Doppler shift in the radiation scattered from the aerosols illuminated by the laser. Because it is a cw focused system, rather than pulsed, it is difficult to extract range information, and its look-ahead is limited to a warning of only a few seconds. In recent years, pulsed transversely excited atmospheric pressure (TEA) CO_2 lasers have been made increasingly reliable for long-term operation. Such a system has been used with good success by R. Michael Hardesty at NOAA to measure wind velocity and map wind fields over a 20-km range with a lidar system located in a van.[9] From these studies it is clear that similar systems using smaller lasers can be developed for airborne applications.

7. Simulation and Performance Analysis of the Ho:YAG and CO_2 Lidars

The approach simulated in our study is that of a pulsed laser which is focused 3 km in front of the aircraft and is then coherently detected to yield the Doppler shift in the light scattered back to the aircraft. A typical optical heterodyne transceiver is shown in Fig. 5. More than 100 lidar simulation runs have been made for NASA by Coherent Technologies, Inc., computing end-to-end signal-to-noise ratios and velocity errors for two candidate lidars as a function of distance from the core of the Dallas/Fort Worth microburst. A simplified form of the

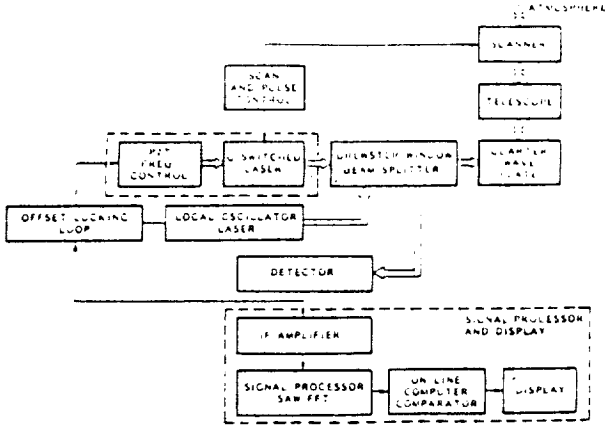

Fig. 5 Typical optical heterodyne transceiver.

lidar equation used for these calculations is shown below.

$$\frac{S}{N} = \frac{\pi E D^2 \beta \lambda \eta K(R)}{8R^2 \quad Bh}$$

where

E	=	laser pulse energy
D	=	telescope diameter
β	=	backscatter cross section
λ	=	laser wavelength
η	=	detection and mixing efficiency
$K(R)$	=	round-trip extinction for range R
R	=	range of return
B	=	system bandwidth
h	=	Planck's constant

Representative results from these analyses are presented by Huffaker.[10] A conclusion of this work is that, in order to demonstrate a windshear threat, it is sufficient for a sensor system to determine that there is a performance-increasing wind followed spatially by a performance-decreasing wind, where these changes are of the order of 10 to 20 knots per half kilometer. An initial assumption has been that 30 s of warning time was a requirement of an airborne windshear-detection system. Using the Ho:YAG or CO_2 lidars examined in this study, this warning time is achievable in most, but not all, microburst situations. In the Dallas/Fort Worth microburst, the peak rain rate was 3.85 in./h at the core. The starting parameters for the two lidars are shown in Table 2.

Table 2. Base-Case Lidar Parameters

Parameters	Lidar System	
	Ho:YAG(2.1 μm)	CO_2(10.6 μm)
500-m Backscatter Coeff. (1/(m-sr))	1.28×10^{-6}	5×10^{-8}
Efficiency ($\eta_T = \eta_o \eta_c \eta_q$)	0.1	0.1
Attenuation (dB/km)	0.1	1.0
Pulse Energy (mJ)	5	5
Bandwidth (MHz)	10	1.0
Pulse Length (μs)	0.5	1.0
Mirror Diameter (cm)	15	15

Using the lidar equation to calculate SNRs, we find that a 5-mJ CO_2 lidar on board an aircraft 4 km from the core center will be able to penetrate approximately 250 m into the core. This lidar will completely sense the performance-increasing portion of the winds, but only the start of the performance-decreasing winds in the 1985 Dallas Fort Worth example.

If an aircraft is 2 km from the microburst core center, the CO_2 lidar can penetrate approximately 700 m into the core of the microburst. This increase in penetration allows the lidar to show clearly a significant portion of the performance-decreasing winds. Reducing the look-ahead distance from 4 km to 2 km reduces the warning time to ~12 s before the aircraft reaches the near "edge" of the microburst. We have examined what energy-increasing strategies a pilot can employ, for example, in a Boeing 727 with 12 s in which to prepare for an encounter with a microburst. If the pilot has confidence in the warning he receives from the lidar-based windshear alarm, he can initiate a "go-around" procedure with the aircraft throttle setting advanced to full thrust and a pitch attitude of 15° at a rate of 4°/s. It is then possible for him to gain 500 ft of altitude within the available 12 s. If the go-around was initiated at an altitude of 400 ft the microburst transit would be accomplished safely. With a warning representative of that which might be obtained with an *in situ* reactive system, the aircraft would not achieve any altitude margin prior to windshear encounter. All of these data were obtained from a simulation carried out on a 727-2A flight simulator, for a plane with gear down and 30° flaps.

Figure 6 shows the signal-to-noise ratio (SNR) as a function of range from the Dallas/Fort Worth microburst for a 5-mJ CO_2 lidar for two aircraft locations. It also shows the radial wind velocity profile associated with this microburst. The Ho:YAG system has a reduced atmospheric attenuation of approximately 0.1 dB/km as compared with 1.0 dB/km for CO_2, as a result of this initially greater SNR, and it has somewhat superior penetration into the rain-filled core of the microburst as compared with CO_2. This performance is shown in

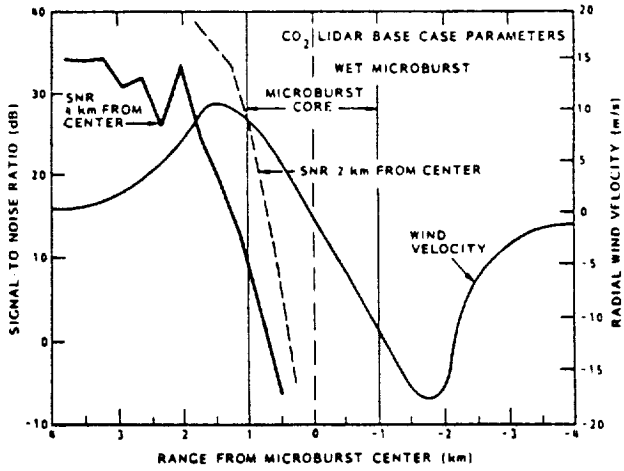

Fig. 6 CO_2 lidar signal-to-noise ratio and true wind velocity versus distance from the microburst core for two aircraft positions, 2 and 4 km from the microburst center.

Fig. 7. The effect of differing SNRs of the 10-μm system is again apparent when we calculate velocity error as a function of range. This calculation is plotted in Fig. 8 for dry-air conditions. The velocity error σ(v) is based on Zrnic's analyses as recently described by Kane.[11]

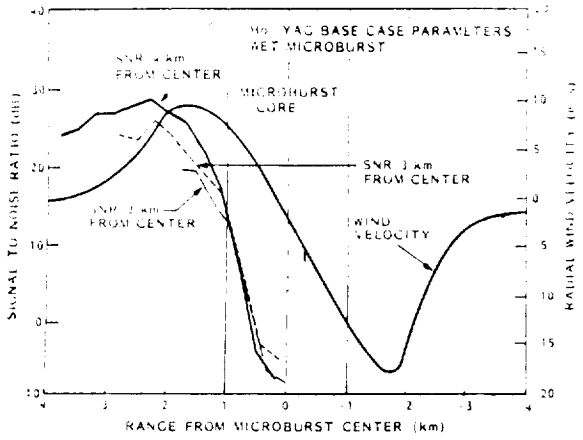

Fig. 7 Ho:YAG lidar signal-to-noise ratio and true wind velocity versus distance from the microburst core for three aircraft positions.

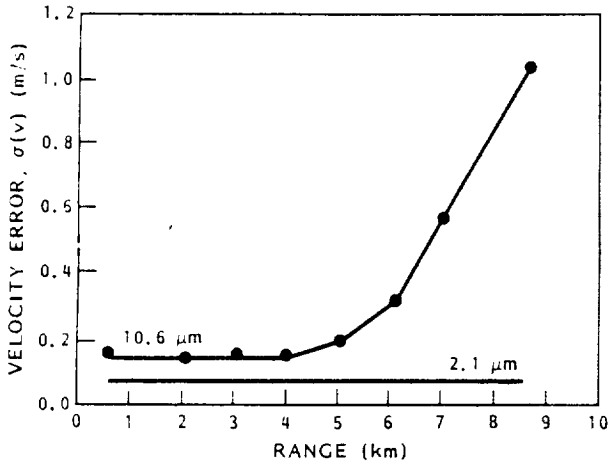

Fig. 8 Comparison of velocity errors for 2.1-μm and 10.6-μm lidars.

8. Lidar Range in Rain and Minimum Required Advance Warning Time

It is well known that lidar has the potential for measuring wind velocity in clear air. One of the overriding concerns of the NASA program has been to determine the performance of lidar systems under conditions of precipitation, both light and heavy. We have made use of the measurements of attenuation in rain by Chu and Hogg[4] and the backscatter measurements of Rensch and Long[11] to calculate the range in rain for unity SNR of our base-case lidar as a function of rain rate. Unity SNR is chosen because the system still has a satisfactory velocity error for that SNR. The data in Fig. 9 show that

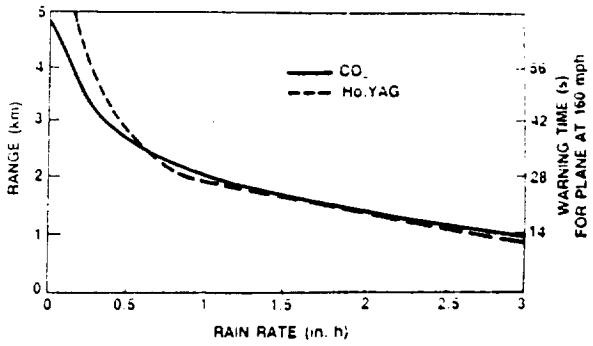

Fig. 9 Range in rain for unity SNR 5-mJ CO_2 and Ho:YAG lidars.

even in a homogeneous rain field of 3 in./h, the base-case lidars can measure wind velocity a kilometer in front of the aircraft. It should be noticed that for moderately heavy rain (2 in./h) both lidar systems have approximately the same penetration capability, 2 km. This is because the attenuation in rain is very large as compared with the differences in the two lidars. At a rain rate of 3 in./h, the round-trip attenuation is −48 dB/km.

The performance degradation of lidars in rain raises several important questions, key among them being, what range of forward-look alert times is required to assure aircraft survivability and flight-crew acceptance of the attendant windshear cockpit automation? A definitive answer to this question is not available at this time, because of the complex issues involving human factors and piloting technique, flight guidance and windshear information display, and considerations of aircraft performance capabilities. Figure 10 shows the change in aircraft energy height accrued from the time of annunciated warning to shear exit, as a function of forward-look

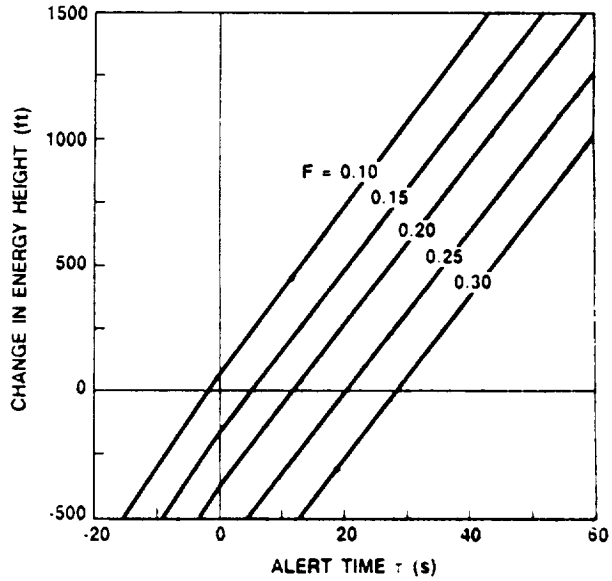

Fig. 10 Change in energy height as a function of forward-look alert time.

alert time, for several values of hazard index F. Negative values of τ represent reactive windshear alerting systems (or no alert at all), whereas positive values of τ represent advanced warning times achievable with remote sensing of atmospheric windshear conditions. Figure 10 clearly demonstrates the benefits and payoff attendant to forward-look windshear detection and warning system concepts. The aircraft selected for this analysis is typical of a modern, medium-range twin turbojet transport. Prior to windshear encounter, the aircraft was assumed to be in approach configuration with a microburst windshear located between the aircraft's current position and the runway threshold. Simplifying assumptions used in the calculations were constant F-factor once the shear is encountered, no change of aircraft configuration, and inclusion of representative latency for engine spool-up characteristics once the crew has elected to execute a windshear escape maneuver. Comparison of Figs. 9 and 10 suggests that lidar performance in moderate to heavy rain is adequate to significantly enhance aircraft survivability, although for short forward-look alert times, complete avoidance of microburst windshear may not be possible. Preliminary results of piloted simulation studies, jointly conducted by Boeing and NASA, tend to confirm the data presented in Fig. 10. Tentative results of the simulator study indicate that short alert times (15 to 30 s) can enable aircraft to attain safe altitude prior to shear entry, and are assessed as timely by the simulator test subjects.

Performance of the Ho:YAG and CO_2 lidar systems has also been evaluated for the "dry" microburst case, of the type typically encountered at Denver/Stapleton Airport. Such a case might include virga, but no rain reaching the ground. Figure 11 shows the SNR for the two lidars, as a function of aircraft distance from the core of the microburst. The true wind velocities are also shown. The velocity error for each system is less than 1 m/s for ranges out to 7 km in front of the aircraft.

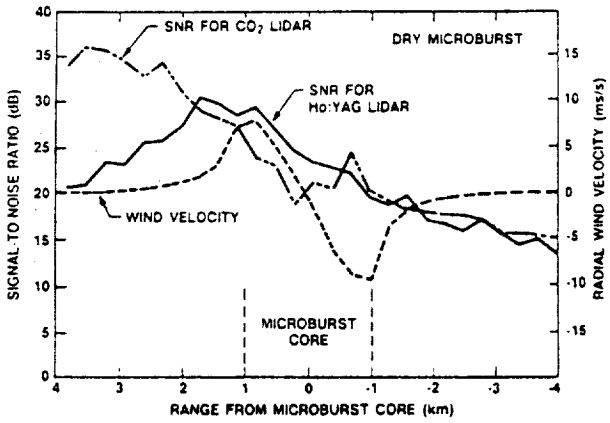

Fig. 11 Signal-to-noise ratio and true wind velocity versus distance from core of a dry microburst.

9. Lidar Hardware Evaluation

One of the goals of the program was to evaluate the state of the art with regard to laser performance and reliability. Together with our subcontractors, Spectra Technology of Seattle, Washington, and Lightwave Electronics of Mountain View, California, we have made detailed performance estimates for CO_2 and Ho:YAG lasers. Both laser systems appear to have the capability to meet the program objectives, with the CO_2 laser having a significant advantage in technical maturity. A 5-mJ radiofrequency pumped waveguide CO_2 laser represents the state of the art for compact, reliable CO_2 lasers and, in the Q-switched mode of operation, appears to be a very low-risk solution to our system requirements. This type of compact, long-lived laser has already demonstrated adequate frequency stability in airborne applications. We have carried out a schematic optomechanical design of an airborne CO_2 lidar using this laser and other commercially available components. The resulting optical package, including laser transmitter, local oscillator, detector, and beam scanner, has a volume of approximately 3 ft^3.

The theoretical performance of the 2-μm lidar appears superior to that of the 10-μm lidar; however, only very low laser output efficiency has been seen to date for room-temperature, Q-switched, 2-μm lasers. There are also several remaining scientific and technological questions for the solid-state 2-μm lidar: (1) Will single-mode oscillation be possible? (2) Will efficient Q-switching be possible? (3) Will practical detectors with adequate frequency response reach the market? (4) Will pump diodes meet their projected lifetime? Efforts were made to identify the potential 2-μm system components together with their likelihood of success, using inputs from the several researchers. Unlike the CO_2 situation, there are no Ho:YAG vendors, only researchers. Therefore, if we had to select which laser system should be incorporated into the windshear lidar today, we would have no choice but to select the 10-μm system. A conceptual design layout for the optical head of an airborne windshear is shown in Fig. 12.

10. Conclusions

Lidar appears to be a viable approach to windshear detection and avoidance, even in conditions of moderately heavy precipitation. The technology necessary to design, build, and test a brassboard 10-μm CO_2 lidar is available. The airborne lidar windshear-detection systems analyzed in this program can give the pilot information about the line-of-sight component of windshear threat from his present position to a region extending 2 to 3 km in front of the aircraft. Techniques to measure and display vertical wind components and spatial distribution are a significant part of the windshear problem, and will be addressed in our continuing investigation. Although an eye-safe lidar at 2 μm enjoys some performance advantages, the lasers and detectors for such a lidar have not yet been sufficiently developed to support their use in a near-term system. In the long term, diode-pumped solid-state lidars could well supplant CO_2.

Although both CO_2 and Ho:YAG systems are shown feasible for airborne windshear detection in this study, several important questions remain to be answered before final decisions on development are made. Specifically, additional simulation studies are needed to investigate techniques to measure both the radial (line-of-sight) and vertical winds. A "dry" microburst case will be examined in the same way the present "wet" microburst was analyzed. Lidar scanning techniques will be investigated to allow modeling of the spatial extent of the threat, as well as radial and vertical components. The signal-processing algorithms to define

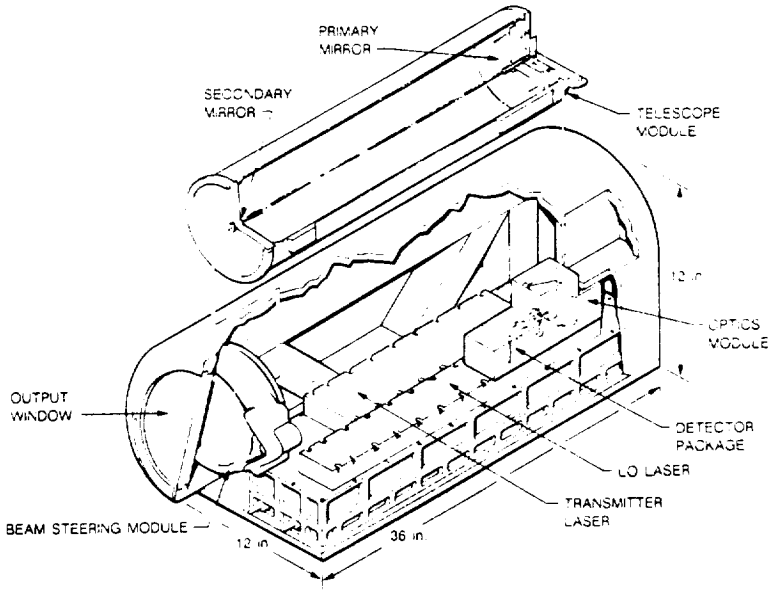

Fig. 12 Conceptual design of an airborne CO_2 laser radar.

the windshear threat must be examined along with recent advances in lidar signal processing. Developments in CO_2 and solid-state technology should continue to be monitored. A more fully developed windshear hazard analysis and warning criterion should be developed and incorporated into the computer simulation.

Finally, some of these questions can be answered definitively only through an airborne sensor-validation program. Such a program would be aimed at determining lidar performance against a windshear threat, characterizing that threat, examining lidar system performance in turbulent flows, and collecting valuable data on windshear phenomenology.

11. References

1. Wilson, J. W., et al., "Microburst Wind Structure and Evaluation of Doppler Radar For Airport Windshear Detection," prepared for the Joint Airport Weather Studies Project. National Center for Atmospheric Research, Boulder, Colorado. NCAR report JAWS, January 1984.

2. Federal Aviation Administration, "Windshear Training Aid," example windshear training program, November 1986.

3. Bowles, R. L., and Frost, W., *Windshear/Turbulence Inputs to Flight Simulation and Systems Certification*. NASA-CP-2474, July 1987.

4. Chu, T. S., and Hogg, D. C., "Effects of Precipitation at 0.63, 3.5, and 10.6 Microns," *The Bell Systems Technical Journal*, May-June 1968.

5. *Airborne Windshear Detection and Warning Systems, First Combined Manufacturers' and Technologists' Conference*, NASA-CP-10006, FAA/PS-88/7, January 1988.

6. Kuhn, P. M., Kurkoski, R. L., and Carasina, F., "Airborne Operation of an Infrared Low-Level Windshear Protection System," *Journal of Aircraft*, Vol. 20, No. 2, February 1983.

7. Bilbro, J. W., "Atmospheric Laser Doppler Velocimetry: An Overview," *Optical Engineering*, Vol. 19, No. 4, July-August 1980.

8. Vaughan, J. M., et al., *Atmospheric Backscatter at 10.6 Microns*, a compendium of measurements made outside the United Kingdom by the Airborne LATAS Coherent Laser Radar Velocimeter. Procurement Ministry of Defense, RSRE, Malvern Worchestershire. May 1987.

9. Hardesty, R. M., et al., "Ground-Based Coherent Lidar Measurement of Tropospheric and Stratospheric Parameters," *SPIE*, Vol. 415, *Coherent Infrared Radar Systems and Applications II*, 1983.

10. Huffaker, R. M., et al., "Performance Analysis and Technical Assessment of Coherent Lidar Systems for Airborne Wind Shear Detection," SPIE Paper 889-11. January 1988.

11. Kane, T. J., Zhou, B., and Byer, R, "Potential for Coherent Wind Velocity Lidar Using Neodymium Lasers," *Applied Optics*, Vol. 23, No. 15, August 1984.

12. Rensch, D. B., and Long, R. K., "Comparative Studies of Extinction and Backscattering by Aerosols, Fog, and Rain at 10.6 μ and 0.63 μ," *Applied Optics*, Vol. 9, No. 7, July 1970.